PROCEEDINGS OF SCIENCE

Novel QCD Phenomena

Stanley J. Brodsky*
Stanford Linear Accelerator Center, Stanford University, Stanford, California 94309
E-mail: sjbth@slac.stanford.edu

I discuss a number of novel topics in QCD, including the use of the AdS/CFT correspondence between Anti-de Sitter space and conformal gauge theories to obtain an analytically tractable approximation to QCD in the regime where the QCD coupling is large and constant. In particular, there is an exact correspondence between the fifth-dimension coordinate z of AdS space and a specific impact variable ζ which measures the separation of the quark constituents within the hadron in ordinary space-time. This connection allows one to compute the analytic form of the frame-independent light-front wavefunctions of mesons and baryons, the fundamental entities which encode hadron properties and allow the computation of exclusive scattering amplitudes. I also discuss a number of novel phenomenological features of QCD. Initial- and final-state interactions from gluon-exchange, normally neglected in the parton model, have a profound effect in QCD hard-scattering reactions, leading to leading-twist single-spin asymmetries, diffractive deep inelastic scattering, diffractive hard hadronic reactions, the breakdown of the Lam Tung relation in Drell-Yan reactions, and nuclear shadowing and non-universal antishadowing — leading-twist physics not incorporated in the light-front wavefunctions of the target computed in isolation. I also discuss tests of hidden color in nuclear wavefunctions, the use of diffraction to materialize the Fock states of a hadronic projectile and test QCD color transparency, and anomalous heavy quark effects. The presence of direct higher-twist processes where a proton is produced in the hard subprocess can explain the large proton-to-pion ratio seen in high centrality heavy ion collisions.

High-pT physics at LHC
March 23-27, 2007
University of Jyväskylä, Jyväskylä, Finland

*Speaker.

PoS(LHC07)002

1. Introduction

Quantum Chromodynamics is a theory with remarkably novel and interesting features. Heavy ion experiments at RHIC [1] are now discovering unexpected new phenomena associated with the high temperature phase of QCD where its quark and gluon degrees of freedom become manifest. Experiments at HERMES [2] have confirmed QCD expectations for leading-twist single-spin asymmetries which require both the presence of quark orbital angular momentum in the proton wavefunction and novel final-state QCD phases. Experiments at HERA [3] have shown that diffractive deep inelastic scattering, where the proton target remains intact, constitutes a remarkably large percentage of the deep inelastic cross section, again showing the importance of QCD final state interactions. The SELEX experiment [4] has shown that single, and even double-charm, hadrons are produced at high x_F in hadron collisions in agreement with analyses based on the intrinsic charm [5] fluctuations of the proton. Color transparency [6], a key feature of the gauge theoretic description of hadron interactions, has now been experimentally established at FermiLab [7] using diffractive dijet production $\pi A \to$ jet jet A. The FermiLab experiment also provides a measurement of the valence light-front wavefunction of the pion [8]. A similar experiment at the LHC $pA \to$ jet jet jet$A$ at the LHC could be used to measure the fundamental valence wavefunction of the proton [9].

The LHC, in both proton-proton and heavy ion collisions, will not only open up a new high energy frontier, but it will also be a superb machine for probing and testing QCD. The advent of new hadron physics accelerators, such as the 12 GeV electron facility at Jefferson Laboratory, the FAIR anti-proton and heavy ion facilities at GSI, and the J-PARC hadron facility will provide many new opportunities to test QCD in its natural domain. In addition, many novel features of QCD, such as timelike deeply virtual Compton scattering and two-photon annihilation, can be probed at electron-positron colliders.

In this talk I will emphasize a number of aspects of QCD which seem to violate conventional wisdom:

(1) As recently noted by Collins and Qiu [10], the traditional factorization formalism of perturbative QCD for high transverse momentum hadron production fails in detail because of initial- and final-state gluonic interactions. These interactions produce the Sivers effect at leading twist [11] with different signs in semi-inclusive deep inelastic scattering and the Drell-Yan reaction [12]. Double initial-state interactions [13] also produce anomalous angular effects, including the breakdown of the Lam-Tung relation [14] in the Drell-Yan process.

(2) Hard diffractive reactions such as diffractive deep inelastic lepton scattering $ep \to epX$ are leading-twist, Bjorken-scaling phenomena. In fact, as shown at HERA [3], nearly 15% of the inclusive deep inelastic cross section leaves the proton intact. This is now understood to be due to final-state gluonic interactions of the struck quark with the proton's spectators [15], contradicting models based on an intrinsic pomeron component of the proton.

(3) As emphasized by Lai, Tung, and Pumplin [16], there are strong indications that the structure functions used to model charm and bottom quarks in the proton at large x_{bj} have been strongly underestimated, since they ignore intrinsic heavy quark fluctuations of hadron wavefunctions. The SELEX [4] discovery of *ccd* and *ccu* double-charm baryons at large x_F reinforces other signals for the presence of heavy quarks at large momentum fractions in hadronic wavefunctions, a rigor-

ous feature of intrinsic heavy quark Fock states. This has strong consequences for the production of heavy hadrons, heavy quarkonia, and even the Higgs at the LHC. Intrinsic charm and bottom leads to substantial rates for heavy hadron production at high x_F [17], as well as anomalous nuclear effects.

(4) The existence of dynamical higher-twist processes in which a hadron interacts directly within a hard subprocess is a rigorous prediction of QCD. For example, in the case of the Drell-Yan reaction $\pi p \to \ell^+\ell^- X$ the virtual photon becomes longitudinally polarized at high x_F , reflecting the spin of the pion entering the QCD hard subprocess [18]. In the case of high transverse momentum proton production the differential cross section $\frac{d\sigma}{d^3p/E}(pp \to ppX)$ scales as $\frac{1}{p_T^8}$ at fixed $x_T = 2p_T/\sqrt{s}$, [19] far from the $1/p_T^4$ to $1/p_T^5$ scaling predicted by pQCD [20]. This suggests that the proton is produced directly in the hard subprocess, rather than by quark or gluon fragmentation. The color transparency [6] of the produced proton and the resulting lack of absorption in a nuclear medium can explain the paradoxical observation seen at RHIC that more protons than pions are produced at high p_T in high centrality heavy ion collisions.

(5) A new understanding of nuclear shadowing and antishadowing has emerged based on the presence of multi-step coherent reactions involving leading twist diffractive reactions [21, 22]. Thus the nuclear shadowing of structure functions is a consequence of the lepton-nucleus collision; it is not an intrinsic property of the nuclear wavefunction. The same analysis shows that antishadowing is *not universal*, but it depends in detail on the flavor of the quark or antiquark constituent [22].

(6) QCD predicts that a nucleus cannot be described solely as nucleonic bound states. In the case of the deuteron, the six-quark wavefunction has five color-singlet components, only one of which can be identified with the *pn* state at long distances. These “hidden color" components [23] play an essential role in nuclear dynamics at short distances.

(7) Spin correlations are now playing an essential role in hadron physics phenomenology, particularly in single-spin correlations which are found to be unexpectedly strong in hadroproduction at large x_F and in the double-spin correlations which measure transversity. One of the most remarkable phenomena in hadron physics is the 4:1 ratio R_{NN} of parallel to antiparallel rates seen in large-angle elastic proton-proton scattering at $E_{cm} \simeq 5$ GeV [24]. This “exclusive transversity" is a possible signal for the existence of $uuduudc\bar{c}$ resonances at the charm threshold [25]. The absence of transverse polarization of the $J\psi$ produced at high transverse momentum in $pp \to J/\psi X$ is a key difficulty for heavy quark phenomenology.

(8) It is commonly believed that the renormalization scale entering the QCD coupling is an arbitrary parameter in perturbative QCD; in fact, just as in Abelian theory, the renormalization scale is a physical quantity, representing the summation of QCD vacuum polarization contributions to the gluon propagator in the skeleton expansion [26]. In general, multiple renormalization scales appear in a pQCD expression whenever multiple invariants appear in the reaction. These issues are discussed in the next section.

These examples of unconventional wisdom highlight the need for a fundamental understanding the dynamics of hadrons in QCD at the amplitude level. This is essential for understanding the description of phenomena such as the quantum mechanics of hadron formation, the remarkable effects of initial and final interactions, the origins of diffractive phenomena and single-spin asym-

metries, and manifestations of higher-twist semi-exclusive hadron subprocesses. A central tool in these analyses is the light-front wavefunctions of hadrons, the frame-independent eigensolutions of the Heisenberg equation for QCD $H^{LF}|\Psi>=M^2|\Psi>$ quantized at fixed light-front. Given the light-front wavefunctions $\psi_{n/H}(x_i,\vec{k}_{\perp i},\lambda_i)$, one can compute a large range of exclusive and inclusive hadron observables. For example, the valence, sea-quark and gluon distributions are defined from the squares of the LFWFS summed over all Fock states n. Form factors, exclusive weak transition amplitudes [27] such as $B\to\ell\nu\pi$, and the generalized parton distributions [28] measured in deeply virtual Compton scattering are (assuming the "handbag" approximation) overlaps of the initial and final LFWFS with $n=n'$ and $n=n'+2$.

I will also discuss here a new approach [29, 30] for determining light-front wavefunctions for QCD using the AdS/CFT correspondence between Anti-de Sitter space and conformal gauge theories. AdS/CFT provides an analytically tractable approximation to QCD in the regime where the QCD coupling is large and constant. In particular, there is an exact correspondence between the fifth-dimension coordinate z of AdS space and a specific impact variable ζ which measures the separation of the quark constituents within the hadron in ordinary space-time. This connection allows one to compute the analytic form of the frame-independent light-front wavefunctions of mesons and baryons, the fundamental entities which encode hadron properties and allow the computation of exclusive scattering amplitudes.

2. Setting the Renormalization Scale in Perturbative QCD

Precise quantitative predictions of QCD are necessary to understand the backgrounds to new beyond-the-Standard-Model phenomena at the LHC . Thus it is important to eliminate as best as possible all uncertainties in QCD predictions, including the elimination of renormalization scale and scheme ambiguities.

It should be emphasized that the renormalization scale is *not arbitrary* in gauge theories. For example in QED, the renormalization scale in the usual Gell Mann-Low scheme is exactly the photon virtuality: $\mu_R^2=k^2$. This scale sums all vacuum polarization corrections into the dressed photon propagator of a given skeleton graph. The resulting analytic QED running coupling has dispersive cuts set correctly set at the physical thresholds for lepton pair production $k^2=4m_L^2$. (In $\overline{MS}$ scheme, the renormalization scales are displaced to $e^{-5/3}k^2$.) The renormalization scale is similarly unambiguous in QCD: the cuts due to quark loops in the dressed gluon propagator appear at the physical quark thresholds. Equivalently, one can use the scheme-independent BLM procedure [26, 31, 32] to eliminate the appearance of the β-function in the perturbative series.

Of course the *initial choice* of the renormalization scale is completely arbitrary, and one can study the dependence of a perturbative expansion on the initial scale using the usual renormalization group evolution equations. This procedure exposes the $\beta-$dependent terms in the PQCD expression. Eliminating the β-dependent terms then leads to a unique, physical, renormalization scale for any choice of renormalization scheme. In effect, one identifies the series for the corresponding conformal theory where the $\beta-$ function is zero; the conformal expression serves as a template [33] for perturbative QCD expansions; the nonzero QCD β-function can then be systematically incorporated into the scale of the running coupling [31, 34, 35]. This leads to fixing of the

physical renormalization scale as well as commensurate scale relations which relate observables to each other without scale or scheme ambiguity [26].

As an example, consider Higgs production $pp \to HX$ calculated via $gg \to H$ fusion. The physical renormalization scale for the running QCD couplings for this subprocess in the pinch scheme are the two gluon virtualities, not the Higgs mass. The resulting values for the renormalization scales parallel the two-photon process in QED: $ee \to eeH$ where only vacuum polarization corrections determine the scale; i.e., the renormalization scales are set by the photon virtualities. An interesting consequence is the prediction that the QCD coupling is evaluated at the minimal scale of the gluon virtualities if the Higgs is measured at $\vec{p}_T^{\,H} = 0$.

In a physical renormalization scheme [36], gauge couplings are defined directly in terms of physical observables. Such effective charges are analytic functions of the physical scales and their mass thresholds have the correct threshold dependence [37, 38] consistent with unitarity. As in QED, heavy particles contribute to physical predictions even at energies below their threshold. This is in contrast to renormalization schemes such as $\overline{MS}$ where mass thresholds are treated as step functions. In the case of supersymmetric grand unification, one finds a number of qualitative differences and improvements in precision over conventional approaches [38]. The analytic threshold corrections can be important in making the measured values of the gauge couplings consistent with unification.

Relations between observables have no scale ambiguity and are independent of the choice of the intermediate renormalization scheme [31]; this is the transitivity property of the renormalization group. The results, called commensurate scale relations, are consistent [39] with the renormalization group [40] and the analytic connection of QCD to Abelian theory at $N_C \to 0$ [41]. A important example is the generalized Crewther relation [34]. One finds a renormalization-scheme invariant relation between the coefficient function for the Bjorken sum rule for polarized deep inelastic scattering and the R-ratio for the e^+e^- annihilation cross section. This relation provides a generalization of the Crewther relation to non-conformally invariant gauge theories. The derived relations allow one to calculate unambiguously without renormalization scale or scheme ambiguity the effective charges of the polarized Bjorken and the Gross-Llewellen Smith sum rules from the experimental value for the effective charge associated with R-ratio. Present data are consistent with the generalized Crewther relations, but measurements at higher precision and energies are needed to decisively test these fundamental relations in QCD.

Recently Michael Binger and I [42] have analyzed the behavior of the thirteen nonzero form factors contributing to the gauge-invariant three-gluon vertex at one-loop, an analysis which is important for setting the renormalization scale for heavy quark production and other PQCD processes. Supersymmetric relations between scalar, quark, and gluon loops contributions to the triangle diagram lead to a simple presentation of the results for a general non-Abelian gauge theories. Only the gluon contribution to the form factors is needed since the massless quark and scalar contributions are inferred from the homogeneous relation $F_G + 4F_Q + (10-d)F_S = 0$ and the sums $\Sigma_{QG}(F) \equiv (d-2)/2F_Q + F_G$ which are given for each form factor F. The extension to the case of internal masses leads to the modified sum rule $F_{MG} + 4F_{MQ} + (9-d)F_{MS} = 0$. The phenomenology of the three-gluon vertex is largely determined by the form factor multiplying the three-level tensor. One can define a three-scale effective scale $Q^2_{eff}(p_a^2, p_b^2, p_c^2)$ as a function of the three external virtualities which provides a natural extension of BLM scale setting [26] to the three-gluon ver-

tex. Physical momentum scales thus set the scale of the coupling. The dependence of Q^2_{eff} on the physical scales has a number of surprising features. A complicated threshold and pseudo-threshold behavior is also observed.

3. AdS/QCD as a First Approximant to Nonperturbative QCD

One of the most interesting new developments in hadron physics has been the application of the AdS/CFT correspondence [43] to nonperturbative QCD problems [44, 45, 46, 47, 48]. Already AdS/CFT is giving important insight into the viscosity and other global properties of the hadronic system formed in heavy ion collisions [49].

The essential ansatz for the application of AdS/CFT to hadron physics is the indication that the QCD coupling $\alpha_s(Q^2)$ becomes large and constant in the low momentum domain $Q \leq 1$ GeV/c, thus providing a window where conformal symmetry can be applied. Solutions of the QCD Dyson Schwinger equations [50, 51] and phenomenological studies [52, 53, 54] of QCD couplings based on physical observables such as τ decay [55] and the Bjorken sum rule show that the QCD β function vanishes and $\alpha_s(Q^2)$ become constant at small virtuality; *i.e.*, effective charges develop an infrared fixed point. Recent lattice gauge theory simulations [56] and nonperturbative analyses [57] have also indicated an infrared fixed point for QCD. One can understand this physically [58]: in a confining theory where gluons have an effective mass or maximal wavelength, all vacuum polarization corrections to the gluon self-energy decouple at long wavelength. When the coupling is constant and quark masses can be ignored, the QCD Lagrangian becomes conformally invariant [59], allowing the mathematically tools of conformal symmetry to be applied.

The leading power fall-off of the hard scattering amplitude as given by dimensional counting rules follows from the conformal scaling of the underlying hard-scattering amplitude: $T_H \sim 1/Q^{n-4}$, where n is the total number of fields (quarks, leptons, or gauge fields) participating in the hard scattering [70, 71]. Thus the reaction is dominated by subprocesses and Fock states involving the minimum number of interacting fields. In the case of $2 \to 2$ scattering processes, this implies $d\sigma/dt(AB \to CD) = F_{AB\to CD}(t/s)/s^{n-2}$, where $n = N_A + N_B + N_C + N_D$ and n_H is the minimum number of constituents of H. The near-constancy of the effective QCD coupling helps explain the empirical success of dimensional counting rules for the near-conformal power law fall-off of form factors and fixed angle scaling [72]. For example, one sees the onset of perturbative QCD scaling behavior even for exclusive nuclear amplitudes such as deuteron photodisintegration (Here $n = 1+6+3+3 = 13$.) $s^{11}d\sigma/dt(\gamma d \to pn) \sim$ constant at fixed CM angle.

The measured deuteron form factor also appears to follow the leading-twist QCD predictions at large momentum transfers in the few GeV region [73, 74, 75].

Recently the Hall A collaboration at Jefferson Laboratory [76] has reported a significant exception to the general empirical success of dimensional counting in fixed CM angle Compton scattering $\frac{d\sigma}{dt}(\gamma p \to \gamma p) \sim \frac{F(\theta_{CM})}{s^8}$ instead of the predicted $\frac{1}{s^6}$ scaling. However, the hadron form factor $R_V(T)$, which multiplies the $\gamma q \to \gamma q$ amplitude is found by Hall-A to scale as $\frac{1}{t^2}$, in agreement with the PQCD and AdS/CFT prediction. In addition the timelike two-photon process $\gamma\gamma \to p\overline{p}$ appears to satisfy dimensional counting [77, 78].

The vanishing of the β function at small momentum transfer implies that there is regime where QCD resembles a strongly-coupled theory and mathematical techniques based on conformal

invariance can be applied. One can use the AdS/CFT correspondence between Anti-de Sitter space and conformal gauge theories to obtain an approximation to nonperturbative QCD in the regime where the QCD coupling is large and constant; i.e., one can use the mathematical representation of the conformal group $SO(4,2)$ in five- dimensional anti-de Sitter space to construct a holographic representation to the theory. For example, Guy de Teramond and I [29] have shown that the amplitude $\Phi(z)$ describing the hadronic state in the fifth dimension of Anti-de Sitter space AdS_5 can be precisely mapped to the light-front wavefunctions $\psi_{n/h}$ of hadrons in physical space-time, thus providing a description of hadrons in QCD at the amplitude level. The light-front wavefunctions are relativistic and frame-independent generalizations of the familiar Schrödinger wavefunctions of atomic physics, but they are determined at fixed light-cone time $\tau = t + z/c$—the "front form" advocated by Dirac—rather than at fixed ordinary time t. We derived this correspondence by noticing that the mapping of $z \to \zeta$ analytically transforms the expression for the form factors in AdS/CFT to the exact Drell-Yan-West expression in terms of light-front wavefunctions.

Conformal symmetry can provide a systematic approximation to QCD in both its nonperturbative and perturbative domains. In the case of nonperturbative QCD, one can use the AdS/CFT correspondence [43] between Anti-de Sitter space and conformal gauge theories to obtain an analytically tractable approximation to QCD in the regime where the QCD coupling is large and constant. Scale-changes in the physical $3+1$ world can then be represented by studying dynamics in a mathematical fifth dimension with the AdS_5 metric. This is illustrated in fig. 1. This connec-

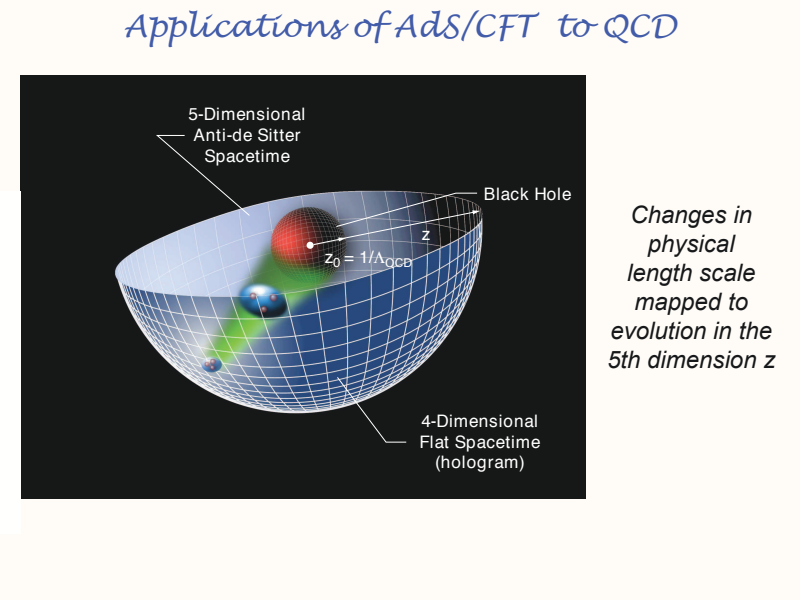

Figure 1: Artist's conception of AdS/CFT. The evolution of the proton at different length scales is mapped into the compact AdS_5 dimension z. The black hole represents the bag-like Dirichlet boundary condition $(\psi(z)|_{z=z_0=1/\Lambda_{QCD}} = 0)$, thus limiting interquark separations.

tion allows one to compute the analytic form [29, 58] of the light-front wavefunctions of mesons and baryons. AdS/CFT also provides a non-perturbative derivation of dimensional counting rules for the power-law fall-off of form factors and exclusive scattering amplitudes at large momentum transfer.

The AdS/CFT approach thus allows one to construct a model of hadrons which has both confinement at large distances and the conformal scaling properties which reproduce dimensional counting rules for hard exclusive reactions. The fundamental equation of AdS/CFT has the appearance of a radial Schrödinger Coulomb equation, but it is relativistic, covariant, and analytically tractable.

A key result from AdS/CFT is an effective two-particle light-front radial equation for mesons [29, 58]

$$\left[-\frac{d^2}{d\zeta^2}+V(\zeta)\right]\phi(\zeta)=\mathscr{M}^2\phi(\zeta), \tag{3.1}$$

with the conformal potential $V(\zeta)=-(1-4L^2)/4\zeta^2$. Here $\zeta^2=x(1-x)\mathbf{b}_\perp^2$ where $x=k^+/P^+$ is the light cone momentum fraction, and $b_\perp$ is the impact separation; i.e. the Fourier conjugate to the relative transverse momentum $k_\perp$. The variable ζ, $0\le\zeta\le\Lambda_{\rm QCD}^{-1}$, represents the invariant separation between point-like constituents, and it is also the holographic variable z in AdS; *i.e.*, we can identify $\zeta=z$. The solution to (3.1) is $\phi(z)=z^{-\frac{3}{2}}\Phi(z)=Cz^{\frac{1}{2}}J_L(z\mathscr{M})$. This equation reproduces the AdS/CFT solutions. The lowest stable state is determined by the Breitenlohner-Freedman bound [60]. We can model confinement by imposing Dirichlet boundary conditions at $\phi(z=1/\Lambda_{\rm QCD})=0$. The eigenvalues are then given in terms of the roots of the Bessel functions: $\mathscr{M}_{L,k}=\beta_{L,k}\Lambda_{\rm QCD}$. Alternatively, one can add a confinement potential $-\kappa^2\zeta^2$ to the effective potential $V(\zeta)$ [47].

The eigenvalues of the effective light-front equation provide a good description of the meson and baryon spectra for light quarks [61], and its eigensolutions provide a remarkably simple but realistic model of their valence wavefunctions. The resulting normalized light-front wavefunctions for the truncated space model are

$$\widetilde{\psi}_{L,k}(x,\zeta)=B_{L,k}\sqrt{x(1-x)}J_L\left(\zeta\beta_{L,k}\Lambda_{\rm QCD}\right)\theta\left(z\le\Lambda_{\rm QCD}^{-1}\right), \tag{3.2}$$

where $B_{L,k}=\pi^{-\frac{1}{2}}\Lambda_{\rm QCD}\ J_{1+L}(\beta_{L,k})$. The results display confinement at large inter-quark separation and conformal symmetry at short distances, thus reproducing dimensional counting rules for hard exclusive processes. One can also derive analogous equations for baryons composed of massless quarks using a Dirac matrix representation for the baryon system. Predictions for the baryon spectrum are shown in fig.2.

Most important, the eigensolutions of the AdS/CFT equation can be mapped to light-front equations of the hadrons in physical space-time, thus providing an elegant description of the light hadrons at the amplitude level. The mapping is illustrated in fig.3. The meson LFWF is illustrated in fig.4. The prediction for the proton Dirac form factor is shown in fig.5.

The deeply virtual Compton amplitudes can be Fourier transformed to $b_\perp$ and $\sigma=x^-P^+/2$ space providing new insights into QCD distributions [62, 63, 64, 65]. The distributions in the LF direction σ typically display diffraction patterns arising from the interference of the initial and final state LFWFs [64, 66]. This is illustrated in fig.6. All of these processes can provide a detailed test of the AdS/CFT LFWFs predictions.

It is interesting to note that the pion distribution amplitude predicted by AdS/CFT at the hadronic scale is $\phi_\pi(x,Q_0)=(4/\sqrt{3}\pi)f_\pi\sqrt{x(1-x)}$ from both the harmonic oscillator and truncated space models is quite different than the asymptotic distribution amplitude predicted from

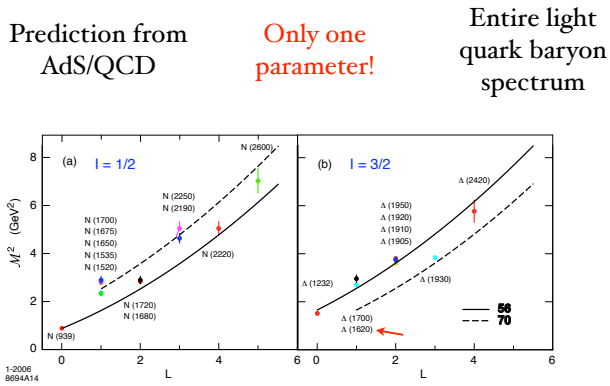

Figure 2: Predictions for the masses of the orbital excitations of the $I = 1/2$ and $I = 3/2$ baryon states from AdS/CFT using the truncated space model. All four-star states listed by the Particle Data Group are shown. Λ_{QCD} =0.25GeV. The 56 trajectory corresponds to L even P = + states, and the 70 to L odd P = - states.

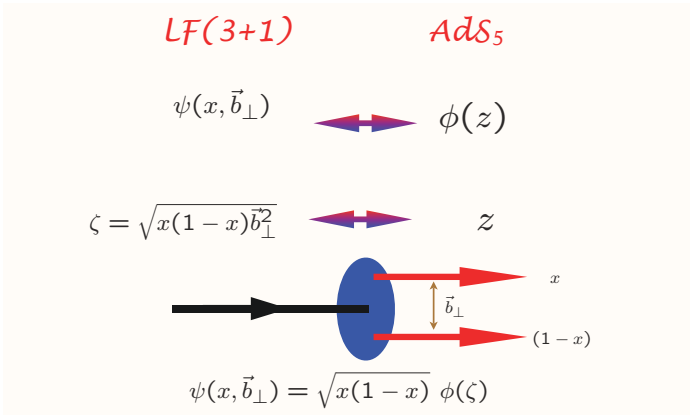

Figure 3: Holographic mapping of the wavefunction $\phi(z)$ in the fifth-dimension coordinate z to the light-front wavefunction as a function of the covariant impact coordinate $\zeta = \sqrt{x(1-x)}b_\perp$.

the PQCD evolution [67] of the pion distribution amplitude: $\phi_\pi(x, Q \to \infty) = \sqrt{3} f_\pi x(1-x)$. The broader shape of the AdS/CFT pion distribution increases the magnitude of the leading-twist perturbative QCD prediction for the pion form factor by a factor of $16/9$ compared to the prediction based on the asymptotic form, bringing the PQCD prediction close to the empirical pion form factor [68]. Hadron form factors can be directly predicted from the overlap integrals in AdS space or equivalently by using the Drell-Yan-West formula in physical space-time. The form factor at high Q^2 receives contributions from small $\zeta \sim 1/Q$, corresponding to small $\vec{b}_\perp$ and $1-x$.

The $x \to 1$ endpoint domain of structure functions is often referred to as a "soft" Feynman contribution. In fact $x \to 1$ for the struck quark requires that all of the spectators have $x = k^+/P^+ = (k^0 + k^z)/P^+ \to 0$; this in turn requires high longitudinal momenta $k^z \to -\infty$ for all spectators – unless one has both massless spectator quarks $m \equiv 0$ with zero transverse momentum $k_\perp \equiv 0$, which is a regime of measure zero. If one uses a covariant formalism, such as the Bethe-Salpeter theory, then the virtuality of the struck quark becomes infinitely spacelike: $k_F^2 \sim -(k_\perp^2 + m^2)/(1-x)$ in the endpoint domain. Thus, actually, $x \to 1$ corresponds to infinite relative longitudinal momentum;

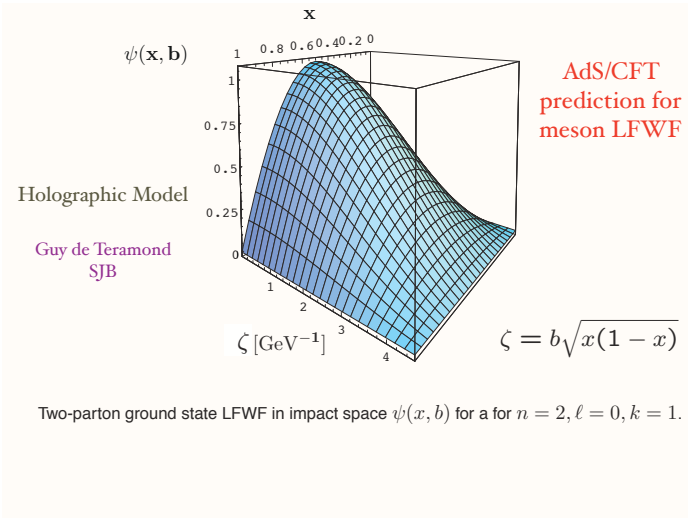

Figure 4: Illustration of the valence $q\bar{q}$ Fock state light-front wavefunction of a meson predicted by AdS/CFT.

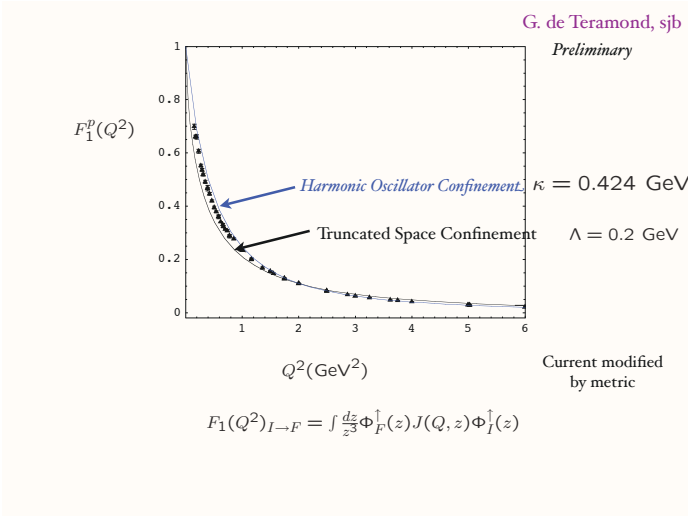

Figure 5: Predictions from AdS/CFT for the space-like Dirac form factor of the proton $F_1(Q^2)$ for both the hard wall (truncated space) and soft wall (harmonic oscillator confinement) models. The current J is modified by the metric. For example, in the soft wall model, $J_\kappa(Q,z) = \Gamma\left(1+\frac{Q^2}{4\kappa^2}\right)U\left(\frac{Q^2}{4\kappa^2},0,\kappa^2 z^2\right)$, where $U(a,b,z)$ is the confluent hypergeometric function [144].

it is as hard a domain in the hadron wavefunction as high transverse momentum. Note also that at large x where the struck quark is far-off shell, DGLAP evolution is quenched [69], so that the fall-off of the DIS cross sections in Q^2 satisfies inclusive-exclusive duality at fixed W^2.

The AdS/CFT approach thus provides a viable, analytic first approximation to QCD. In principle, the model can be systematically improved, for example by using the AdS/CFT eigensolutions as a basis for diagonalizing the full QCD Hamiltonian. An outline of the AdS/QCD program is shown in fig.8. The phenomenology of the AdS/CFT model is just beginning, but it can be anticipated that it will have many applications to LHC phenomena. For example, the model LFWFs

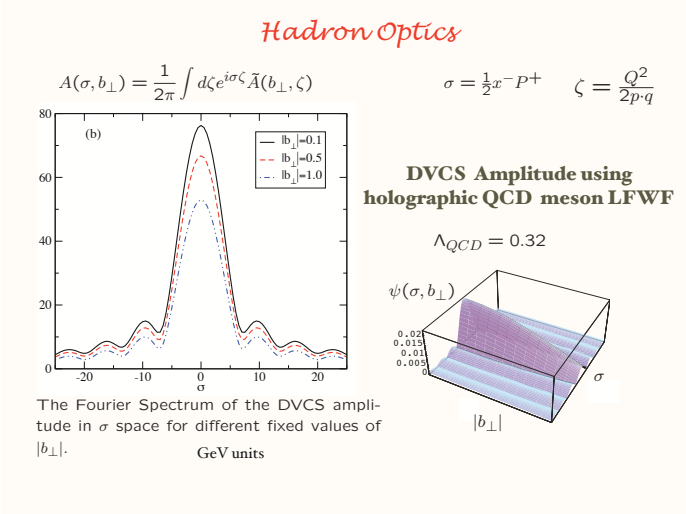

Figure 6: The Fourier transform of the skewness ξ distribution of the generalized parton distribution predicted by AdS/CFT, giving information of the hadron in the light-front coordinate $\sigma = x^- P^+/2$ [64].

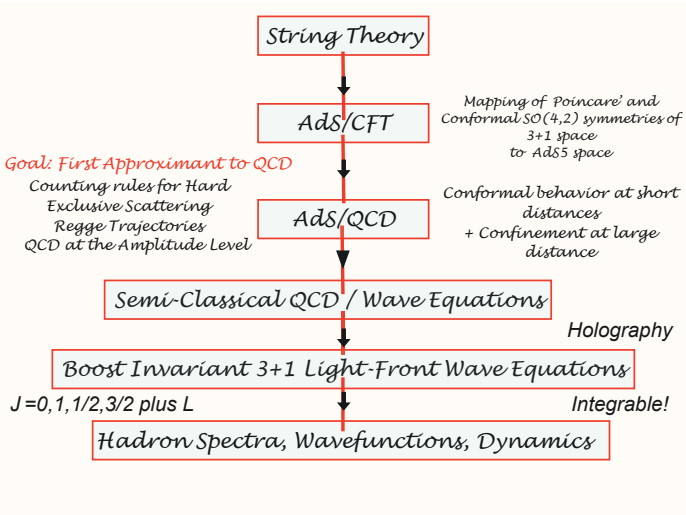

Figure 7: The logistics of AdS/CFT which leads to an analytic first approximation to QCD in its conformal window.

provide a basis for understanding hadron structure functions and fragmentation functions at the amplitude level; the same wavefunctions can describe hadron formation from the coalescence of co-moving quarks. The spin correlations which underly single and double spin correlations are also described by the AdS/CFT eigensolutions. The AdS/CFT hadronic wavefunctions provides predictions for the generalized parton distributions and weak decay amplitudes from first principles. In addition, a prediction from AdS/CFT for the proton LFWF would allow one to compute the higher-twist direct subprocesses such as $uu \to p\bar{d}$ which could control proton production in inclusive reactions at large transverse momenta from first principles. The amplitudes relevant to diffractive reactions could also be computed. We also anticipate that the extension of the AdS/CFT formalism to heavy quarks will allow a great variety of heavy hadron phenomena to be analyzed

from first principles.

4. Higher-Twist Contributions to Inclusive Reactions

Although the contributions of higher twist processes are nominally power-law suppressed at high transverse momentum, there are some phenomenological examples where they can play a dominant role. For example, hadrons can interact directly within a hard subprocess, leading to higher twist contributions which can actually dominate over leading twist processes [18, 79]. A classic example is the reaction $\pi q \to \ell^+\ell^- q'$ which, despite its relative $\frac{1}{Q^2}$ fall-off, dominates the leading twist contribution to the Drell-Yan reaction $\pi N \to \ell^+\ell^- X$ at high x_F, producing longitudinally polarized lepton pairs. Crossing predicts that one also has reactions where the final-state hadron appears directly in the subprocess such as $e^+e^- \to \pi X$ at $z = 1$.

The fundamental test of leading-twist QCD predictions in high transverse momentum hadronic reactions is the measurement of the power-law fall-off of the inclusive cross section $\frac{d\sigma}{d^3p/E}(AB \to CX) = \frac{F(\theta_{cm},x_T)}{p_T^{n_{eff}}}$ at fixed $x_T = 2p_T/\sqrt{s}$ and fixed θ_{CM} where $n_{eff} \sim 4 + \delta$. Here $\delta \leq 1$ is the correction to the conformal prediction arising from the QCD running coupling and DGLAP evolution of the input distribution and fragmentation functions [20]. Striking deviations from the leading-twist predictions were observed at the ISR and Fermilab fixed-target experiments [80]. For example, the Chicago-Princeton experiment [81] found $n_{eff} \simeq 12$ for $pp \to pX$ at large, fixed x_T. A compilation of results for the power fall-off for hard inclusive hadronic reactions is shown in fig.8.

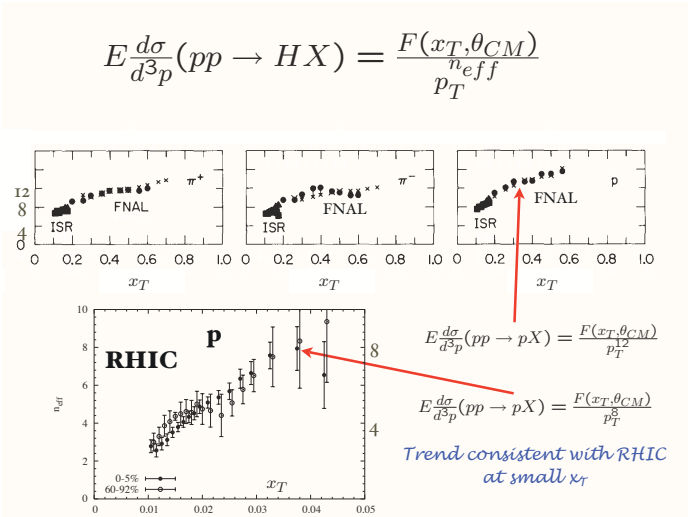

Figure 8: Power-law scaling [82] for hadron production at large transverse momentum from experiments at the ISR, FermiLab, and the PHENIX collaboration at RHIC. The leading-twist prediction is $n_{eff} \simeq 4$. The $n_{eff} \sim 8$ scaling behavior observed at RHIC for both $pA \to pX$ and $AA \to pX$ at $x_T > 0.03$ is consistent with the dominance of a higher-twist direct process.

It is conventional to assume that leading-twist subprocesses dominate measurements of high p_T hadron production at RHIC energies. Indeed the data for direct photon fragmentation $pp \to \gamma X$ is quite consistent with $n_{eff}(pp \to \gamma X) = 5$, as expected from the $gq \to \gamma q$ leading-twist subprocess. This also is likely true for pion production, at least for small x_T. However, the measured fixed

x_T scaling for proton production at RHIC is anomalous: PHENIX reports $n_{eff}(pp \to pX) \simeq 8$. A review of this data is given by Tannenbaum [82]. One can understand the anomalous scaling if a higher-twist subprocess [20] , where the proton is made *directly* within the hard reaction such as $uu \to p\bar{d}$ and $(uud)u \to pu$, dominate the reaction $pp \to pX$ at RHIC energies. This is illustrated in fig.11. Such processes are rigorous QCD contributions. The dominance of direct subprocesses

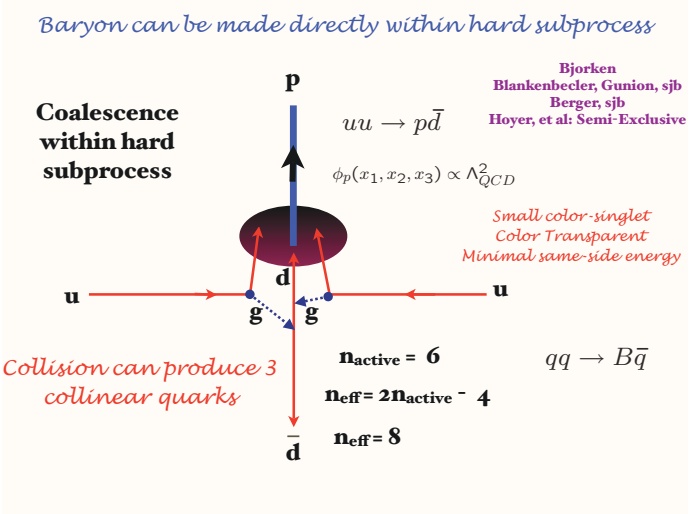

Figure 9: Representative higher-twist mechanism for direct proton production at large transverse momentum based on the subprocess $uu \to p\bar{d}$. The cross section scales as $E\frac{d\sigma}{d^3p} = \frac{F(x_T,\theta_{CM})}{p_T^{n_{eff}}}$ where $n_{eff} = 8$.

is possible since the fragmentation of gluon or quark jets to baryons requires that the 2 to 2 subprocess occurs at much higher transverse momentum than the p_T of observed proton because of the fast falling $(1-z)^3$ quark-to-proton fragmentation function. Such "direct" reactions can readily explain the fast-falling power-law falloff observed at fixed x_T and fixed-θ_{cm} observed at the ISR, FermiLab and RHIC [20]. Furthermore, the protons produced directly within the hard subprocess emerge as small-size color-transparent colored states which are not absorbed in the nuclear target. In contrast, pions produced from jet fragmentation have the normal cross section. This provides a plausible explanation of RHIC data [83], which shows a dramatic rise of the $p \to \pi$ ratio at high p_T when one compares peripheral with central (full overlap) heavy ion collisions. This is illustrated in fig.10. The directly produced protons are not absorbed, but the pions are diminished in the nuclear medium.

5. Intrinsic Heavy Quarks and the Anomalous Nuclear Dependence of Quarkonium Production

The probability for Fock states of a light hadron such as the proton to have an extra heavy quark pair decreases as $1/m_Q^2$ in non-Abelian gauge theory [84, 85]. The relevant matrix element is the cube of the QCD field strength $G^3_{\mu\nu}$. This is in contrast to abelian gauge theory where the relevant operator is $F^4_{\mu\nu}$ and the probability of intrinsic heavy leptons in QED bound state is suppressed as $1/m_\ell^4$. The intrinsic Fock state probability is maximized at minimal off-shellness. It

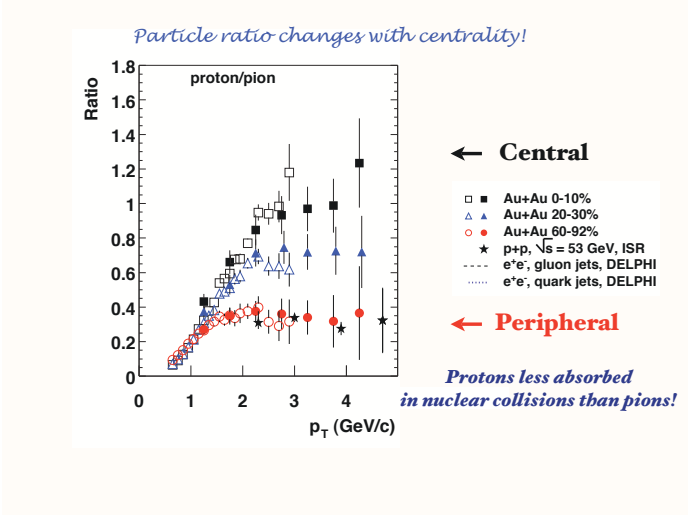

Figure 10: The ratio of protons to pions produced at large p_T in heavy ion collisions as a function of centrality from the PHENIX experiment at RHIC [83]. The open and solid symbols indicate neutral versus charged pions. The rise of the p/π ratio with p_T is consistent with the hypothesis that only the pions are absorbed in the nuclear medium. A comparison with the measured p/π ratio in e^+e^- and pp reactions is also shown.

is useful to define the transverse mass $m_{\perp i} = \sqrt{k_{\perp i}^2 + m_i^2}$. The maximum probability then occurs at $x_i = m_\perp^i / \sum_{j=1}^n m_\perp^j$; *i.e.*, when the constituents have minimal invariant mass and equal rapidity. Thus the heaviest constituents have the highest momentum fractions and the highest x_i. Intrinsic charm thus predicts that the charm structure function has support at large x_{bj} in excess of DGLAP extrapolations [5]; this is in agreement with the EMC measurements [86]. Intrinsic charm can also explain the $J/\psi \to \rho\pi$ puzzle [87]. It also affects the extraction of suppressed CKM matrix elements in B decays [88].

The dissociation of the intrinsic charm $|uudc\bar{c}>$ Fock state of the proton on a nucleus can produce a leading heavy quarkonium state at high $x_F = x_c + x_{\bar{c}}$ in $pA \to J/\psi XA'$ since the c and $\bar{c}$ can readily coalesce into the charmonium state. Since the constituents of a given intrinsic heavy-quark Fock state tend to have the same rapidity, coalescence of multiple partons from the projectile Fock state into charmed hadrons and mesons is also favored. For example, one can produce a leading Λ_c at high x_F and low p_T from the coalescence of the udc constituents of the projectile $|uudc\bar{c}>$ Fock state. A similar coalescence mechanism was used in atomic physics to produce relativistic antihydrogen in $\bar{p}A$ collisions [89]. This phenomena is important not only for understanding heavy-hadron phenomenology, but also for understanding the sources of neutrinos in astrophysics experiments [90] and the "long-flying" component in cosmic rays [91].

In the case of a nuclear target, the charmonium state will be produced at small transverse momentum and high x_F with a characteristic $A^{2/3}$ nuclear dependence since the color-octet color-octet $|(uud)_{8C}(c\bar{c})_{8C}>$ Fock state interacts on the front surface of the nuclear target [17]. This forward contribution is in addition to the A^1 contribution derived from the usual perturbative QCD fusion contribution at small x_F. Because of these two components, the cross section violates perturbative QCD factorization for hard inclusive reactions [92]. This is consistent with the observed

two-component cross section for charmonium production observed by the NA3 collaboration at CERN [93] and more recent experiments [94]. The diffractive dissociation of the intrinsic charm Fock state leads to leading charm hadron production and fast charmonium production in agreement with measurements [95]. Intrinsic charm can also explain the $J/\psi \to \rho\pi$ puzzle [87], and it affects the extraction of suppressed CKM matrix elements in B decays [88].

The production cross section for the double-charm Ξ_{cc}^{+} baryon [96] and the production of J/ψ pairs appears to be consistent with the diffractive dissociation and coalescence of double IC Fock states [97]. These observations provide compelling evidence for the diffractive dissociation of complex off-shell Fock states of the projectile and contradict the traditional view that sea quarks and gluons are always produced perturbatively via DGLAP evolution. It is also conceivable that the observations [98] of Λ_b at high x_F at the ISR in high energy pp collisions could be due to the diffractive dissociation and coalescence of the "intrinsic bottom" $|uudb\bar{b}>$ Fock states of the proton.

Intrinsic heavy quarks can also enhance the production probability of Higgs bosons at hadron colliders from processes such as $gc \to Hc$. It is thus critical for new experiments (HERMES, HERA, COMPASS) to definitively establish the phenomenology of the charm structure function at large x_{bj}. Recently Kopeliovich, Schmidt, Soffer, and I [17] have proposed a novel mechanism for exclusive diffractive Higgs production $pp \to pHp$ in which the Higgs boson carries a significant fraction of the projectile proton momentum. The production mechanism is based on the subprocess $(Q\overline{Q})g \to H$ where the $Q\overline{Q}$ in the $|uudQ\overline{Q}>$ intrinsic heavy quark Fock state has up to 80% of the projectile protons momentum. This process, which is illustrated in fig.11, will provide a clear experimental signal for Higgs production due to the small background in this kinematic region.

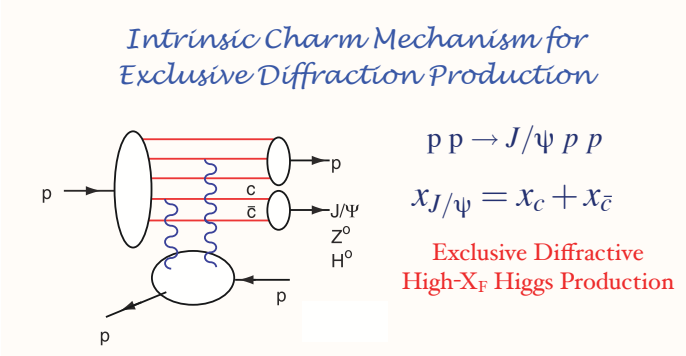

Figure 11: Intrinsic charm mechanism for doubly diffractive high x_F Higgs, Z^0 and J/ψ production.

6. Hidden Color

In traditional nuclear physics, the deuteron is a bound state of a proton and a neutron where the binding force arise from the exchange of a pion and other mesonic states. However, QCD provides a new perspective: [99, 100] six quarks in the fundamental 3_C representation of $SU(3)$ color can combine into five different color-singlet combinations, only one of which corresponds to a proton and neutron. In fact, if the deuteron wavefunction is a proton-neutron bound state at large distances, then as their separation becomes smaller, the QCD evolution resulting from colored gluon exchange

introduce four other "hidden color" states into the deuteron wavefunction [23]. The normalization of the deuteron form factor observed at large Q^2 [101], as well as the presence of two mass scales in the scaling behavior of the reduced deuteron form factor [99], thus suggest sizable hidden-color Fock state contributions such as $|(uud)_{8_C}(ddu)_{8_C}\rangle$ with probability of order 15% in the deuteron wavefunction [102].

The hidden color states of the deuteron can be materialized at the hadron level as $\Delta^{++}(uuu)\Delta^{-}(ddd)$ and other novel quantum fluctuations of the deuteron. These dual hadronic components become more and more important as one probes the deuteron at short distances, such as in exclusive reactions at large momentum transfer. For example, the ratio $d\sigma/dt(\gamma d \to \Delta^{++}\Delta^{-})/d\sigma/dt(\gamma d \to np)$ should increase dramatically to a fixed ratio 2 :: 5 with increasing transverse momentum p_T. Similarly the Coulomb dissociation of the deuteron into various exclusive channels $ed \to e' + pn, pp\pi^-, \Delta\Delta, \cdots$ should have a changing composition as the final-state hadrons are probed at high transverse momentum, reflecting the onset of hidden color degrees of freedom.

Recently the CLEO collaboration [103] has measured the branching ratios of $\Upsilon(nS) \to$ antideuteron X. This reaction should be sensitive to the hidden-color structure of the anti-deuteron wavefunction since the $\Upsilon \to b\bar{b} \to ggg \to qqqqqq\overline{qqqqqq}$ originates from a system of small compact size and leads to multi-quark states with diverse colors. It is crucial to also have data on $\Upsilon \to \overline{pn}X$ where the anti-nucleons emerge at minimal invariant mass. The conventional nuclear physics expectation can then be computed from the convolution of this distribution with the square of the two nucleon "body" LFWF of the deuteron:

$$\int d^2k_\perp \int_0^1 dx |\psi^{\bar{d}}_{\overline{np}}(x,k_\perp)|^2 \times \frac{d\sigma}{d^3p_{\bar{n}}/E_{\bar{n}}\, d^3p_{\bar{p}}/E_{\bar{p}}}(\Upsilon \to \overline{np}X) \tag{6.1}$$

7. Diffractive Deep Inelastic Scattering

A remarkable feature of deep inelastic lepton-proton scattering at HERA is that approximately 10% events are diffractive [104, 105]: the target proton remains intact, and there is a large rapidity gap between the proton and the other hadrons in the final state. These diffractive deep inelastic scattering (DDIS) events can be understood most simply from the perspective of the color-dipole model: the $q\bar{q}$ Fock state of the high-energy virtual photon diffractively dissociates into a diffractive dijet system. The exchange of multiple gluons between the color dipole of the $q\bar{q}$ and the quarks of the target proton neutralizes the color separation and leads to the diffractive final state. The same multiple gluon exchange also controls diffractive vector meson electroproduction at large photon virtuality [106]. This observation presents a paradox: if one chooses the conventional parton model frame where the photon light-front momentum is negative $q+ = q^0 + q^z < 0$, the virtual photon interacts with a quark constituent with light-cone momentum fraction $x = k^+/p^+ = x_{bj}$. Furthermore, the gauge link associated with the struck quark (the Wilson line) becomes unity in light-cone gauge $A^+ = 0$. Thus the struck "current" quark apparently experiences no final-state interactions. Since the light-front wavefunctions $\psi_n(x_i, k_{\perp i})$ of a stable hadron are real, it appears impossible to generate the required imaginary phase associated with pomeron exchange, let alone large rapidity gaps.

This paradox was resolved by Hoyer, Marchal, Peigne, Sannino and myself [15]. Consider the case where the virtual photon interacts with a strange quark—the $s\bar{s}$ pair is assumed to be produced in the target by gluon splitting. In the case of Feynman gauge, the struck s quark continues to interact in the final state via gluon exchange as described by the Wilson line. The final-state interactions occur at a light-cone time $\Delta\tau \simeq 1/\nu$ shortly after the virtual photon interacts with the struck quark. When one integrates over the nearly-on-shell intermediate state, the amplitude acquires an imaginary part. Thus the rescattering of the quark produces a separated color-singlet $s\bar{s}$ and an imaginary phase. In the case of the light-cone gauge $A^+ = \eta \cdot A = 0$, one must also consider the final-state interactions of the (unstruck) $\bar{s}$ quark. The gluon propagator in light-cone gauge $d^{\mu\nu}_{LC}(k) = (i/k^2 + i\varepsilon)\,[-g^{\mu\nu} + (\eta^\mu k^\nu + k^\mu \eta^\nu/\eta\cdot k)]$ is singular at $k^+ = \eta\cdot k = 0$. The momentum of the exchanged gluon k^+ is of $\mathcal{O}(1/\nu)$; thus rescattering contributes at leading twist even in light-cone gauge. The net result is gauge invariant and is identical to the color dipole model calculation. The calculation of the rescattering effects on DIS in Feynman and light-cone gauge through three loops is given in detail for an Abelian model in reference [15]. The result shows that the rescattering corrections reduce the magnitude of the DIS cross section in analogy to nuclear shadowing.

A new understanding of the role of final-state interactions in deep inelastic scattering has thus emerged. The multiple scattering of the struck parton via instantaneous interactions in the target generates dominantly imaginary diffractive amplitudes, giving rise to an effective “hard pomeron" exchange. The presence of a rapidity gap between the target and diffractive system requires that the target remnant emerges in a color-singlet state; this is made possible in any gauge by the soft rescattering. The resulting diffractive contributions leave the target intact and do not resolve its quark structure; thus there are contributions to the DIS structure functions which cannot be interpreted as parton probabilities [15]; the leading-twist contribution to DIS from rescattering of a quark in the target is a coherent effect which is not included in the light-front wave functions computed in isolation. One can augment the light-front wave functions with a gauge link corresponding to an external field created by the virtual photon $q\bar{q}$ pair current [107, 108]. Such a gauge link is process dependent [12], so the resulting augmented LFWFs are not universal [15, 107, 109]. We also note that the shadowing of nuclear structure functions is due to the destructive interference between multi-nucleon amplitudes involving diffractive DIS and on-shell intermediate states with a complex phase. In contrast, the wave function of a stable target is strictly real since it does not have on-energy-shell intermediate state configurations. The physics of rescattering and shadowing is thus not included in the nuclear light-front wave functions, and a probabilistic interpretation of the nuclear DIS cross section is precluded.

Rikard Enberg, Paul Hoyer, Gunnar Ingelman and I [110] have shown that the quark structure function of the effective hard pomeron has the same form as the quark contribution of the gluon structure function. The hard pomeron is not an intrinsic part of the proton; rather it must be considered as a dynamical effect of the lepton-proton interaction. Our QCD-based picture also applies to diffraction in hadron-initiated processes. The rescattering is different in virtual photon- and hadron-induced processes due to the different color environment, which accounts for the observed non-universality of diffractive parton distributions. This framework also provides a theoretical basis for the phenomenologically successful Soft Color Interaction (SCI) model [111] which includes rescattering effects and thus generates a variety of final states with rapidity gaps.

8. Single-Spin Asymmetries from Final-State Interactions

Among the most interesting polarization effects are single-spin azimuthal asymmetries in semi-inclusive deep inelastic scattering, representing the correlation of the spin of the proton target and the virtual photon to hadron production plane: $\vec{S}_p \cdot \vec{q} \times \vec{p}_H$. Such asymmetries are time-reversal odd, but they can arise in QCD through phase differences in different spin amplitudes. In fact, final-state interactions from gluon exchange between the outgoing quarks and the target spectator system lead to single-spin asymmetries in semi-inclusive deep inelastic lepton-proton scattering which are not power-law suppressed at large photon virtuality Q^2 at fixed x_{bj} [11]. In contrast to the SSAs arising from transversity and the Collins fragmentation function, the fragmentation of the quark into hadrons is not necessary; one predicts a correlation with the production plane of the quark jet itself. Physically, the final-state interaction phase arises as the infrared-finite difference of QCD Coulomb phases for hadron wave functions with differing orbital angular momentum. See fig.12. The same proton matrix element which determines the spin-orbit correlation $\vec{S} \cdot \vec{L}$ also produces the anomalous magnetic moment of the proton, the Pauli form factor, and the generalized parton distribution E which is measured in deeply virtual Compton scattering. Thus the contribution of each quark current to the SSA is proportional to the contribution $\kappa_{q/p}$ of that quark to the proton target's anomalous magnetic moment $\kappa_p = \sum_q e_q \kappa_{q/p}$ [11, 112]. The HERMES collaboration has recently measured the SSA in pion electroproduction using transverse target polarization [2]. The Sivers and Collins effects can be separated using planar correlations; both contributions are observed to contribute, with values not in disagreement with theory expectations [2, 113]. A related analysis also predicts that the initial-state interactions from gluon exchange between the incoming quark and the target spectator system lead to leading-twist single-spin asymmetries in the Drell-Yan process $H_1 H_2^{\uparrow} \to \ell^+ \ell^- X$ [12, 114]. The SSA in the Drell-Yan process is the same as that obtained in SIDIS, with the appropriate identification of variables, but with the opposite sign. There is no Sivers effect in charged-current reactions since the W only couples to left-handed quarks [115].

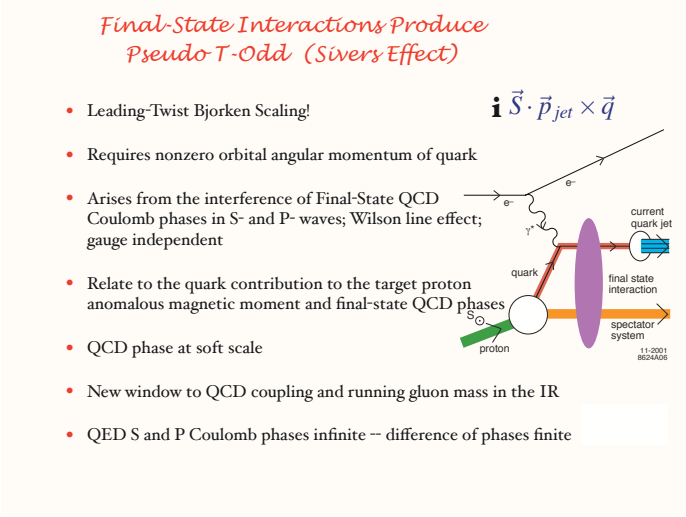

Figure 12: Final-state interactions in QCD and the physics of the leading-twist Sivers single-spin asymmetry in semi-inclusive deep inelastic lepton-proton scattering.

If both the quark and antiquark in the initial state of the Drell-Yan subprocess $q\bar{q} \to \mu^+\mu^-$ interact with the spectators of the other incident hadron, one finds a breakdown of the Lam-Tung relation, which was formerly believed to be a general prediction of leading-twist QCD. These double initial-state interactions also lead to a $\cos 2\phi$ planar correlation in unpolarized Drell-Yan reactions [13]. More generally one must consider subprocesses involving initial-state gluons such as $ngq\bar{q} \to \ell\bar{\ell}$ in addition to subprocesses with extra final-state gluons.

The final-state interaction mechanism provides an appealing physical explanation within QCD of single-spin asymmetries. Remarkably, the same matrix element which determines the spin-orbit correlation $\vec{S}\cdot\vec{L}$ also produces the anomalous magnetic moment of the proton, the Pauli form factor, and the generalized parton distribution E which is measured in deeply virtual Compton scattering. Physically, the final-state interaction phase arises as the infrared-finite difference of QCD Coulomb phases for hadron wave functions with differing orbital angular momentum. An elegant discussion of the Sivers effect including its sign has been given by Burkardt [112]. As shown recently by Gardner and myself [116], one can also use the Sivers effect to study the orbital angular momentum of gluons by tagging a gluon jet in semi-inclusive DIS. In this case, the final-state interactions are enhanced by the large color charge of the gluons.

The final-state interaction effects can also be identified with the gauge link which is present in the gauge-invariant definition of parton distributions [108]. Even when the light-cone gauge is chosen, a transverse gauge link is required. Thus in any gauge the parton amplitudes need to be augmented by an additional eikonal factor incorporating the final-state interaction and its phase [117, 107]. The net effect is that it is possible to define transverse momentum dependent parton distribution functions which contain the effect of the QCD final-state interactions.

9. Diffraction Dissociation as a Tool to Resolve Hadron Substructure and Test Color Transparency

Diffractive multi-jet production in heavy nuclei provides a novel way to resolve the shape of light-front Fock state wave functions and test color transparency [6]. For example, consider the reaction [118, 119]. $\pi A \to \mathrm{Jet}_1 + \mathrm{Jet}_2 + A'$ at high energy where the nucleus A' is left intact in its ground state. The transverse momenta of the jets balance so that $\vec{k}_{\perp i} + \vec{k}_{\perp 2} = \vec{q}_\perp < R^{-1}{}_A$. Because of color transparency, the valence wave function of the pion with small impact separation will penetrate the nucleus with minimal interactions, diffracting into jet pairs [118]. The $x_1 = x$, $x_2 = 1-x$ dependence of the dijet distributions will thus reflect the shape of the pion valence light-cone wave function in x; similarly, the $\vec{k}_{\perp 1} - \vec{k}_{\perp 2}$ relative transverse momenta of the jets gives key information on the second transverse momentum derivative of the underlying shape of the valence pion wavefunction [119, 120]. The diffractive nuclear amplitude extrapolated to $t = 0$ should be linear in nuclear number A if color transparency is correct. The integrated diffractive rate will then scale as $A^2/R_A^2 \sim A^{4/3}$. This is in fact what has been observed by the E791 collaboration at FermiLab for 500 GeV incident pions on nuclear targets [121]. The measured momentum fraction distribution of the jets with high transverse momentum is found to be approximately consistent with the shape of the pion asymptotic distribution amplitude, $\phi_\pi^{\mathrm{asympt}}(x) = \sqrt{3} f_\pi x(1-x)$ [8]; however, there is an indication from the data that the distribution is broader at lower transverse momentum, consistent with the AdS/CFT prediction.

Color transparency, as evidenced by the Fermilab measurements of diffractive dijet production, implies that a pion can interact coherently throughout a nucleus with minimal absorption, in dramatic contrast to traditional Glauber theory based on a fixed $\sigma_{\pi n}$ cross section. Color transparency gives direct validation of the gauge interactions of QCD. Color transparency has also been observed in diffractive electroproduction of ρ mesons [122] and in quasi-elastic $pA \to pp(A-1)$ scattering [123] where only the small size fluctuations of the hadron wavefunction enters the hard exclusive scattering amplitude. In the latter case an anomaly occurs at $\sqrt{s} \simeq 5$ GeV, most likely signaling a resonance effect at the charm threshold [25].

10. Shadowing and Antishadowing of Nuclear Structure Functions

One of the novel features of QCD involving nuclei is the *antishadowing* of the nuclear structure functions which is observed in deep inelastic lepton scattering and other hard processes. Empirically, one finds $R_A(x,Q^2) \equiv \big(F_{2A}(x,Q^2)/(A/2)F_d(x,Q^2)\big) > 1$ in the domain $0.1 < x < 0.2$; *i.e.*, the measured nuclear structure function (referenced to the deuteron) is larger than than the scattering on a set of A independent nucleons.

The shadowing of the nuclear structure functions: $R_A(x,Q^2) < 1$ at small $x < 0.1$ can be readily understood in terms of the Gribov-Glauber theory. Consider a two-step process in the nuclear target rest frame. The incoming $q\bar{q}$ dipole first interacts diffractively $\gamma^* N_1 \to (q\bar{q})N_1$ on nucleon N_1 leaving it intact. This is the leading-twist diffractive deep inelastic scattering (DDIS) process which has been measured at HERA to constitute approximately 10% of the DIS cross section at high energies. The $q\bar{q}$ state then interacts inelastically on a downstream nucleon N_2 : $(q\bar{q})N_2 \to X$. The phase of the pomeron-dominated DDIS amplitude is close to imaginary, and the Glauber cut provides another phase i, so that the two-step process has opposite phase and destructively interferes with the one-step DIS process $\gamma * N_2 \to X$ where N_1 acts as an unscattered spectator. The one-step and-two step amplitudes can coherently interfere as long as the momentum transfer to the nucleon N_1 is sufficiently small that it remains in the nuclear target; *i.e.*, the Ioffe length [124] $L_I = 2M\nu/Q^2$ is large compared to the inter-nucleon separation. In effect, the flux reaching the interior nucleons is diminished, thus reducing the number of effective nucleons and $R_A(x,Q^2) < 1$.

There are also leading-twist diffractive contributions $\gamma^* N_1 \to (q\bar{q})N_1$ arising from Reggeon exchanges in the t-channel [21]. For example, isospin–non-singlet $C = +$ Reggeons contribute to the difference of proton and neutron structure functions, giving the characteristic Kuti-Weisskopf $F_{2p} - F_{2n} \sim x^{1-\alpha_R(0)} \sim x^{0.5}$ behavior at small x. The x dependence of the structure functions reflects the Regge behavior $\nu^{\alpha_R(0)}$ of the virtual Compton amplitude at fixed Q^2 and $t = 0$. The phase of the diffractive amplitude is determined by analyticity and crossing to be proportional to $-1 + i$ for $\alpha_R = 0.5$, which together with the phase from the Glauber cut, leads to *constructive* interference of the diffractive and nondiffractive multi-step nuclear amplitudes. Furthermore, because of its x dependence, the nuclear structure function is enhanced precisely in the domain $0.1 < x < 0.2$ where antishadowing is empirically observed. The strength of the Reggeon amplitudes is fixed by the fits to the nucleon structure functions, so there is little model dependence.

As noted above, the Bjorken-scaling diffractive contribution to DIS arises from the rescattering of the struck quark after it is struck (in the parton model frame $q^+ \leq 0$), an effect induced by the

Wilson line connecting the currents. Thus one cannot attribute DDIS to the physics of the target nucleon computed in isolation [15]. Similarly, since shadowing and antishadowing arise from the physics of diffraction, we cannot attribute these phenomena to the structure of the nucleus itself: shadowing and antishadowing arise because of the $\gamma^* A$ collision and the history of the $q\overline{q}$ dipole as it propagates through the nucleus.

Ivan Schmidt, Jian-Jun Yang, and I [22] have extended the Glauber analysis to the shadowing and antishadowing of all of the electroweak structure functions. Quarks of different flavors will couple to different Reggeons; this leads to the remarkable prediction that nuclear antishadowing is not universal; it depends on the quantum numbers of the struck quark. This picture implies substantially different antishadowing for charged and neutral current reactions, thus affecting the extraction of the weak-mixing angle θ_W. We find that part of the anomalous NuTeV result [125] for θ_W could be due to the non-universality of nuclear antishadowing for charged and neutral currents. Detailed measurements of the nuclear dependence of individual quark structure functions are thus needed to establish the distinctive phenomenology of shadowing and antishadowing and to make the NuTeV results definitive. Schmidt, Yang, and I have also identified contributions to the nuclear multi-step reactions which arise from odderon exchange and hidden color degrees of freedom in the nuclear wavefunction. There are other ways in which this new view of antishadowing can be tested; antishadowing can also depend on the target and beam polarization.

Acknowledgments

Presented at the Workshop, “High-pT physics at the LHC", March 23-27, 2007 in Jyväskylä, Finland. I thank the organizers for their invitation especially Professor Jan Rak, to speak at this workshop. I also thank my collaborators for many helpful discussions. This work was supported in part by the Department of Energy, contract No. DE-AC02-76SF00515.

References

[1] J. W. Harris, Czech. J. Phys. **55**, B297 (2005).

[2] A. Airapetian *et al.* [HERMES Collaboration], Phys. Rev. Lett. **94**, 012002 (2005) [arXiv:hep-ex/0408013].

[3] M. Derrick *et al.* [ZEUS Collaboration], Phys. Lett. B **315**, 481 (1993).

[4] J. S. Russ, Int. J. Mod. Phys. A **21**, 5482 (2006).

[5] S. J. Brodsky, P. Hoyer, C. Peterson and N. Sakai, Phys. Lett. B **93**, 451 (1980).

[6] S. J. Brodsky and A. H. Mueller, Phys. Lett. B **206**, 685 (1988).

[7] D. Ashery, *Talk given at Particles and Nuclei International Conference (PANIC 05), Santa Fe, New Mexico, 24-28 Oct 2005*

[8] E. M. Aitala *et al.* [E791 Collaboration], Phys. Rev. Lett. **86**, 4768 (2001) [arXiv:hep-ex/0010043].

[9] L. Frankfurt, G. A. Miller and M. Strikman, SPIRES entry *Prepared for Exclusive Processes at High Momentum Transfer, Newport News, Virginia, 15-18 May 2002*

[10] J. Collins and J. W. Qiu, arXiv:0705.2141 [hep-ph].

[11] S. J. Brodsky, D. S. Hwang and I. Schmidt, Int. J. Mod. Phys. A **18**, 1327 (2003) [Phys. Lett. B **530**, 99 (2002)] [arXiv:hep-ph/0201296].

[12] J. C. Collins, Phys. Lett. B **536**, 43 (2002) [arXiv:hep-ph/0204004].

[13] D. Boer, S. J. Brodsky and D. S. Hwang, Phys. Rev. D **67**, 054003 (2003) [arXiv:hep-ph/0211110].

[14] C. S. Lam and W. K. Tung, Phys. Rev. D **21**, 2712 (1980).

[15] S. J. Brodsky, P. Hoyer, N. Marchal, S. Peigne and F. Sannino, Phys. Rev. D **65**, 114025 (2002) [arXiv:hep-ph/0104291].

[16] J. Pumplin, H. L. Lai and W. K. Tung, Phys. Rev. D **75**, 054029 (2007) [arXiv:hep-ph/0701220].

[17] S. J. Brodsky, B. Kopeliovich, I. Schmidt and J. Soffer, Phys. Rev. D **73**, 113005 (2006) [arXiv:hep-ph/0603238].

[18] E. L. Berger and S. J. Brodsky, Phys. Rev. Lett. **42**, 940 (1979).

[19] B. I. Abelev *et al.* [STAR Collaboration], arXiv:nucl-ex/0703040.

[20] S. J. Brodsky and M. Rijssenbeek, arXiv:hep-ph/0511178.

[21] S. J. Brodsky and H. J. Lu, Phys. Rev. Lett. **64**, 1342 (1990).

[22] S. J. Brodsky, I. Schmidt and J. J. Yang, Phys. Rev. D **70**, 116003 (2004) [arXiv:hep-ph/0409279].

[23] S. J. Brodsky, C. R. Ji and G. P. Lepage, Phys. Rev. Lett. **51**, 83 (1983).

[24] G. R. Court *et al.*, Phys. Rev. Lett. **57**, 507 (1986).

[25] S. J. Brodsky and G. F. de Teramond, Phys. Rev. Lett. **60**, 1924 (1988).

[26] S. J. Brodsky, G. P. Lepage and P. B. Mackenzie, Phys. Rev. D **28**, 228 (1983).

[27] S. J. Brodsky and D. S. Hwang, Nucl. Phys. B **543**, 239 (1999) [arXiv:hep-ph/9806358].

[28] S. J. Brodsky, M. Diehl and D. S. Hwang, Nucl. Phys. B **596**, 99 (2001) [arXiv:hep-ph/0009254].

[29] S. J. Brodsky, Eur. Phys. J. A **31**, 638 (2007) [arXiv:hep-ph/0610115].

[30] H. R. Grigoryan and A. V. Radyushkin, arXiv:0706.1543 [hep-ph].

[31] S. J. Brodsky and H. J. Lu, Phys. Rev. D **51**, 3652 (1995) [arXiv:hep-ph/9405218].

[32] J. Rathsman, Phys. Rev. D **54**, 3420 (1996) [arXiv:hep-ph/9605401].

[33] S. J. Brodsky and J. Rathsman, arXiv:hep-ph/9906339.

[34] S. J. Brodsky, G. T. Gabadadze, A. L. Kataev and H. J. Lu, Phys. Lett. B **372**, 133 (1996) [arXiv:hep-ph/9512367].

[35] S. J. Brodsky, E. Gardi, G. Grunberg and J. Rathsman, Phys. Rev. D **63**, 094017 (2001) [arXiv:hep-ph/0002065].

[36] G. Grunberg, Phys. Rev. D **29**, 2315 (1984).

[37] S. J. Brodsky, M. S. Gill, M. Melles and J. Rathsman, Phys. Rev. D **58**, 116006 (1998) [arXiv:hep-ph/9801330].

[38] M. Binger and S. J. Brodsky, Phys. Rev. D **69**, 095007 (2004) [arXiv:hep-ph/0310322].

[39] S. J. Brodsky and H. J. Lu, arXiv:hep-ph/9211308.

[40] E. C. G. Stueckelberg and A. Petermann, Helv. Phys. Acta **26**, 499 (1953).

[41] S. J. Brodsky and P. Huet, Phys. Lett. B **417**, 145 (1998) [arXiv:hep-ph/9707543].

[42] M. Binger and S. J. Brodsky, Phys. Rev. D **74**, 054016 (2006) [arXiv:hep-ph/0602199].

[43] J. M. Maldacena, Adv. Theor. Math. Phys. **2**, 231 (1998) [Int. J. Theor. Phys. **38**, 1113 (1999)] [arXiv:hep-th/9711200].

[44] J. Polchinski and M. J. Strassler, Phys. Rev. Lett. **88**, 031601 (2002) [arXiv:hep-th/0109174].

[45] R. A. Janik and R. Peschanski, Nucl. Phys. B **565**, 193 (2000) [arXiv:hep-th/9907177].

[46] J. Erlich, E. Katz, D. T. Son and M. A. Stephanov, Phys. Rev. Lett. **95**, 261602 (2005) [arXiv:hep-ph/0501128].

[47] A. Karch, E. Katz, D. T. Son and M. A. Stephanov, Phys. Rev. D **74**, 015005 (2006) [arXiv:hep-ph/0602229].

[48] G. F. de Teramond and S. J. Brodsky, Phys. Rev. Lett. **94**, 201601 (2005) [arXiv:hep-th/0501022].

[49] P. Kovtun, D. T. Son and A. O. Starinets, Phys. Rev. Lett. **94**, 111601 (2005) [arXiv:hep-th/0405231].

[50] L. von Smekal, R. Alkofer and A. Hauck, Phys. Rev. Lett. **79**, 3591 (1997) [arXiv:hep-ph/9705242].

[51] D. Zwanziger, Phys. Rev. D **69**, 016002 (2004) [arXiv:hep-ph/0303028].

[52] A. C. Mattingly and P. M. Stevenson, Phys. Rev. D **49**, 437 (1994) [arXiv:hep-ph/9307266].

[53] S. J. Brodsky, S. Menke, C. Merino and J. Rathsman, Phys. Rev. D **67**, 055008 (2003) [arXiv:hep-ph/0212078].

[54] M. Baldicchi and G. M. Prosperi, Phys. Rev. D **66**, 074008 (2002) [arXiv:hep-ph/0202172].

[55] S. J. Brodsky, J. R. Pelaez and N. Toumbas, Phys. Rev. D **60**, 037501 (1999) [arXiv:hep-ph/9810424].

[56] S. Furui and H. Nakajima, arXiv:hep-lat/0612009.

[57] D. Antonov and H. J. Pirner, arXiv:hep-ph/0702227.

[58] S. J. Brodsky and G. F. de Teramond, arXiv:hep-th/0702205.

[59] G. Parisi, Phys. Lett. B **39**, 643 (1972).

[60] P. Breitenlohner and D. Z. Freedman, Annals Phys. **144**, 249 (1982).

[61] S. J. Brodsky and G. F. de Teramond, AIP Conf. Proc. **814**, 108 (2006) [arXiv:hep-ph/0510240].

[62] M. Burkardt, Int. J. Mod. Phys. A **21**, 926 (2006) [arXiv:hep-ph/0509316].

[63] X. d. Ji, Phys. Rev. Lett. **91**, 062001 (2003) [arXiv:hep-ph/0304037].

[64] S. J. Brodsky, D. Chakrabarti, A. Harindranath, A. Mukherjee and J. P. Vary, Phys. Lett. B **641**, 440 (2006) [arXiv:hep-ph/0604262].

[65] P. Hoyer, AIP Conf. Proc. **904**, 65 (2007) [arXiv:hep-ph/0608295].

[66] S. J. Brodsky, D. Chakrabarti, A. Harindranath, A. Mukherjee and J. P. Vary, Phys. Rev. D **75**, 014003 (2007) [arXiv:hep-ph/0611159].

[67] G. P. Lepage and S. J. Brodsky, Phys. Lett. B **87**, 359 (1979).

[68] H. M. Choi and C. R. Ji, Phys. Rev. D **74**, 093010 (2006) [arXiv:hep-ph/0608148].

[69] S. J. Brodsky and G. P. Lepage, "Exclusive Processes And The Exclusive Inclusive Connection In Quantum Chromodynamics," CITATION = C79-02-13-1;

[70] S. J. Brodsky and G. R. Farrar, Phys. Rev. D **11**, 1309 (1975).

[71] V. A. Matveev, R. M. Muradian and A. N. Tavkhelidze, Lett. Nuovo Cim. **7**, 719 (1973).

[72] S. J. Brodsky and G. P. Lepage, Adv. Ser. Direct. High Energy Phys. **5**, 93 (1989).

[73] R. J. Holt, Phys. Rev. C **41**, 2400 (1990).

[74] C. Bochna *et al.* [E89-012 Collaboration], Phys. Rev. Lett. **81**, 4576 (1998) [arXiv:nucl-ex/9808001].

[75] P. Rossi *et al.* [CLAS Collaboration], arXiv:hep-ph/0405207.

[76] A. Danagoulian *et al.* [Hall A Collaboration], Phys. Rev. Lett. **98**, 152001 (2007) [arXiv:nucl-ex/0701068].

[77] A. Chen, SPIRES entry *Prepared for International Conference on the Structure and Interactions of the Photon and 14th International Workshop on Photon-Photon Collisions (Photon 2001), Ascona, Switzerland, 2-7 Sep 2001*

[78] A. E. Chen [BELLE Collaboration], Int. J. Mod. Phys. A **21**, 5543 (2006).

[79] E. L. Berger and S. J. Brodsky, Phys. Rev. D **24**, 2428 (1981).

[80] D. W. Sivers, S. J. Brodsky and R. Blankenbecler, Phys. Rept. **23**, 1 (1976).

[81] D. Antreasyan, J. W. Cronin, H. J. Frisch, M. J. Shochet, L. Kluberg, P. A. Piroue and R. L. Sumner, Phys. Rev. D **19**, 764 (1979).

[82] M. J. Tannenbaum, arXiv:nucl-ex/0611008.

[83] S. S. Adler *et al.* [PHENIX Collaboration], Phys. Rev. Lett. **91**, 172301 (2003) [arXiv:nucl-ex/0305036].

[84] M. Franz, M. V. Polyakov and K. Goeke, Phys. Rev. D **62**, 074024 (2000) [arXiv:hep-ph/0002240].

[85] S. J. Brodsky, J. C. Collins, S. D. Ellis, J. F. Gunion and A. H. Mueller,

[86] B. W. Harris, J. Smith and R. Vogt, Nucl. Phys. B **461**, 181 (1996) [arXiv:hep-ph/9508403].

[87] S. J. Brodsky and M. Karliner, Phys. Rev. Lett. **78**, 4682 (1997) [arXiv:hep-ph/9704379].

[88] S. J. Brodsky and S. Gardner, Phys. Rev. D **65**, 054016 (2002) [arXiv:hep-ph/0108121].

[89] C. T. Munger, S. J. Brodsky and I. Schmidt, Phys. Rev. D **49**, 3228 (1994).

[90] F. Halzen, Nucl. Phys. Proc. Suppl. **136**, 93 (2004) [Acta Phys. Polon. B **36**, 481 (2005 APCPC,745,3-13.2005 NUPHA,A752,3-13.2005)] [arXiv:astro-ph/0402083].

[91] I. M. Dremin and V. I. Yakovlev, Astropart. Phys. **26**, 1 (2006) [arXiv:hep-ph/0510377].

[92] P. Hoyer, M. Vanttinen and U. Sukhatme, Phys. Lett. B **246**, 217 (1990).

[93] J. Badier *et al.* [NA3 Collaboration], Phys. Lett. B **104**, 335 (1981).

[94] M. J. Leitch *et al.* [FNAL E866/NuSea collaboration], Phys. Rev. Lett. **84**, 3256 (2000) [arXiv:nucl-ex/9909007].

[95] J. C. Anjos, J. Magnin and G. Herrera, Phys. Lett. B **523**, 29 (2001) [arXiv:hep-ph/0109185].

[96] A. Ocherashvili *et al.* [SELEX Collaboration], Phys. Lett. B **628**, 18 (2005) [arXiv:hep-ex/0406033].

[97] R. Vogt and S. J. Brodsky, Phys. Lett. B **349**, 569 (1995) [arXiv:hep-ph/9503206].

[98] G. Bari *et al.*, Nuovo Cim. A **104**, 1787 (1991).

[99] S. J. Brodsky and B. T. Chertok, Phys. Rev. D **14**, 3003 (1976).

[100] V. A. Matveev and P. Sorba, Lett. Nuovo Cim. **20**, 435 (1977).

[101] R. G. Arnold *et al.*, Phys. Rev. Lett. **35**, 776 (1975).

[102] G. R. Farrar, K. Huleihel and H. y. Zhang, Phys. Rev. Lett. **74**, 650 (1995).

[103] D. M. Asner *et al.* [CLEO Collaboration], Phys. Rev. D **75**, 012009 (2007) [arXiv:hep-ex/0612019].

[104] C. Adloff *et al.* [H1 Collaboration], Z. Phys. C **76**, 613 (1997) [arXiv:hep-ex/9708016].

[105] J. Breitweg *et al.* [ZEUS Collaboration], Eur. Phys. J. C **6**, 43 (1999) [arXiv:hep-ex/9807010].

[106] S. J. Brodsky, L. Frankfurt, J. F. Gunion, A. H. Mueller and M. Strikman, Phys. Rev. D **50**, 3134 (1994) [arXiv:hep-ph/9402283].

[107] A. V. Belitsky, X. Ji and F. Yuan, Nucl. Phys. B **656**, 165 (2003) [arXiv:hep-ph/0208038].

[108] J. C. Collins and A. Metz, Phys. Rev. Lett. **93**, 252001 (2004) [arXiv:hep-ph/0408249].

[109] J. C. Collins, Acta Phys. Polon. B **34**, 3103 (2003) [arXiv:hep-ph/0304122].

[110] S. J. Brodsky, R. Enberg, P. Hoyer and G. Ingelman, Phys. Rev. D **71**, 074020 (2005) [arXiv:hep-ph/0409119].

[111] A. Edin, G. Ingelman and J. Rathsman, Phys. Lett. B **366**, 371 (1996) [arXiv:hep-ph/9508386].

[112] M. Burkardt, Nucl. Phys. Proc. Suppl. **141**, 86 (2005) [arXiv:hep-ph/0408009].

[113] H. Avakian and L. Elouadrhiri [CLAS Collaboration], AIP Conf. Proc. **698**, 612 (2004).

[114] S. J. Brodsky, D. S. Hwang and I. Schmidt, Nucl. Phys. B **642**, 344 (2002) [arXiv:hep-ph/0206259].

[115] S. J. Brodsky, D. S. Hwang and I. Schmidt, Phys. Lett. B **553**, 223 (2003) [arXiv:hep-ph/0211212].

[116] S. J. Brodsky and S. Gardner, Phys. Lett. B **643**, 22 (2006) [arXiv:hep-ph/0608219].

[117] X. d. Ji and F. Yuan, Phys. Lett. B **543**, 66 (2002) [arXiv:hep-ph/0206057].

[118] G. Bertsch, S. J. Brodsky, A. S. Goldhaber and J. F. Gunion, Phys. Rev. Lett. **47**, 297 (1981).

[119] L. Frankfurt, G. A. Miller and M. Strikman, Found. Phys. **30**, 533 (2000) [arXiv:hep-ph/9907214].

[120] N. N. Nikolaev, W. Schafer and G. Schwiete, Phys. Rev. D **63**, 014020 (2001) [arXiv:hep-ph/0009038].

[121] E. M. Aitala *et al.* [E791 Collaboration], Phys. Rev. Lett. **86**, 4773 (2001) [arXiv:hep-ex/0010044].

[122] A. B. Borisov [HERMES Collaboration], Nucl. Phys. A **711**, 269 (2002).

[123] J. L. S. Aclander *et al.*, Phys. Rev. C **70**, 015208 (2004) [arXiv:nucl-ex/0405025].

[124] B. L. Ioffe, Phys. Lett. B **30**, 123 (1969).

[125] G. P. Zeller *et al.* [NuTeV Collaboration], Phys. Rev. Lett. **88**, 091802 (2002) [Erratum-ibid. **90**, 239902 (2003)] [arXiv:hep-ex/0110059].

[126] S. J. Brodsky, arXiv:hep-ph/0004211.

[127] S. J. Brodsky and B. Q. Ma, Phys. Lett. B **381**, 317 (1996) [arXiv:hep-ph/9604393].

[128] S. Kretzer, arXiv:hep-ph/0408287.

[129] B. Portheault, arXiv:hep-ph/0406226.

[130] F. Olness *et al.*, Eur. Phys. J. C **40**, 145 (2005) [arXiv:hep-ph/0312323].

[131] J. Rathsman, in *Proc. of the 5th International Symposium on Radiative Corrections (RADCOR 2000)* ed. Howard E. Haber, arXiv:hep-ph/0101248.

[132] G. Grunberg, JHEP **0108**, 019 (2001) [arXiv:hep-ph/0104098].

[133] T. Banks and A. Zaks, Nucl. Phys. B **196**, 189 (1982).

[134] G. P. Lepage and S. J. Brodsky, Phys. Rev. D **22**, 2157 (1980).

[135] R. J. Crewther, Phys. Rev. Lett. **28**, 1421 (1972).

[136] S. J. Brodsky, Y. Frishman, G. P. Lepage and C. T. Sachrajda, Phys. Lett. B **91**, 239 (1980).

[137] S. J. Brodsky, P. Damgaard, Y. Frishman and G. P. Lepage, Phys. Rev. D **33**, 1881 (1986).

[138] S. J. Brodsky, Y. Frishman and G. P. Lepage, Phys. Lett. B **167**, 347 (1986).

[139] V. M. Braun, G. P. Korchemsky and D. Mueller, Prog. Part. Nucl. Phys. **51**, 311 (2003) [arXiv:hep-ph/0306057].

[140] S. J. Brodsky, arXiv:hep-ph/0408069.

[141] S. J. Brodsky, "Conformal aspects of QCD,"

[142] S. J. Brodsky, "Exclusive processes in quantum chromodynamics and the light-cone Fock representation,"

[143] B. Andersson, G. Gustafson, G. Ingelman and T. Sjostrand, Phys. Rept. **97**, 31 (1983).

[144] S. J. Brodsky and G. F. de Teramond to be published.